CrystEngComm

ROYAL SOCIETY OF CHEMISTRY

COMMUNICATION

View Article Online
View Journal

Check for updates

Cite this: DOI: 10.1039/c8ce00911b

Received 1st June 2018,
Accepted 30th July 2018

DOI: 10.1039/c8ce00911b

rsc.li/crystengcomm

Reversible transformation between $CsPbBr_3$ and Cs_4PbBr_6 nanocrystals†

Yanxiu Li, He Huang, * Yuan Xiong,
Stephen V. Kershaw and Andrey L. Rogach *

A reversible transformation between $CsPbBr_3$ and Cs_4PbBr_6 nanocrystals through a simple treatment with extra ligands or $PbBr_2$ (for the reverse direction) is reported. These transformations are so far the first report of direct reversibility, without a net change in morphology, between $CsPbBr_3$ and Cs_4PbBr_6 and then back to $CsPbBr_3$ nanocrystals, which provides a mechanism for flexible reorganization of the lead halide perovskite lattice.

Since the first colloidal synthesis of lead halide perovskite nanocrystals (NCs) was reported in 2014,[1] the interest in this class of materials has significantly increased.[2–13] Among them, the all-inorganic $CsPbX_3$ perovskite NCs introduced by Kovalenko's group are one of the most promising candidates owing to their high photoluminescence quantum yield (PL QY) reaching almost 100% in solution, easy preparation, and narrow emission peaks.[2,6,14–17] These outstanding properties provide great potential for light-emitting devices with saturated color output,[18–25] photodetectors,[26–30] and lasers.[31,32] There still remain limitations in the understanding of the growth mechanism, formation, and surface properties of different lead halide perovskite NC polymorphs that requires active exploration.[15] For $CsPbX_3$ NCs, the morphology changes related to the dynamic surface ligands binding during the synthesis have been systematically reported by Pan *et al.* and De Roo *et al.*[33,34] The perovskite family of materials is not solely restricted to ABX_3 structures; Cs_4PbX_6 and $CsPb_2X_5$ are examples of alternate perovskites, and these other modifications may not necessarily lend themselves to emissive applications.[35–39] Manna's group reported the synthesis of non-emissive Cs_4PbBr_6 and demonstrated how those materials can be converted to obtain $CsPbX_3$ NCs by the addition of $PbBr_2$.[35] The same group further reported post-synthetic transformation of Cs_4PbBr_6 NCs into $CsPbBr_3$ by physical or chemical extraction of CsBr.[36] CsBr can also be extracted *via* an interfacial reaction with water in a two phase mixture.[37] The amine- and thiol-mediated extraction of $PbBr_2$ from $CsPbX_3$ NCs has been reported to yield Cs_4PbBr_6 NCs.[38,39] $CsPbX_3$ to $CsPb_2X_5$ conversion has been demonstrated through insertion of $PbBr_2$.[35,36] All the reported conversion pathways between $CsPbX_3$ and Cs_4PbX_6 NCs and *vice versa* were so far processed in just one-direction, and necessitated a follow-up purification process including centrifugation and redispersion before further steps. Of direct relevance to the present work, Udayabhaskararao *et al.* showed a phase transformation between $CsPbX_3$ and Cs_4PbX_6 NCs driven by ligand passivation.[40] However and most notably, they transformed

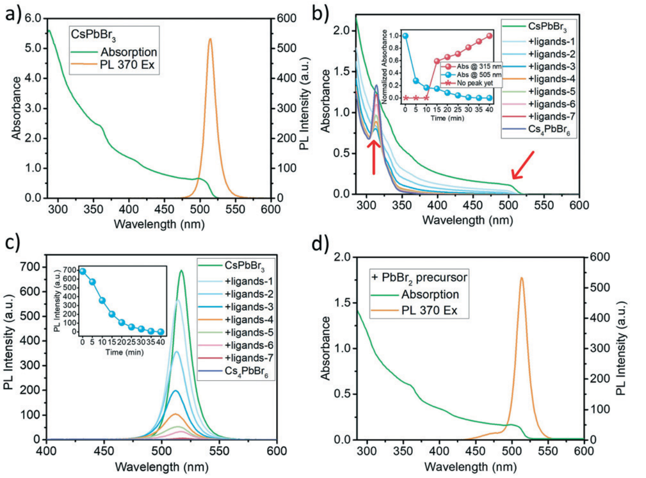

Fig. 1 (a) Absorption and PL spectra of the as-prepared $CsPbBr_3$ NCs, (b) UV-vis absorption monitoring of the transformation progression from $CsPbBr_3$ NCs to Cs_4PbBr_6 NCs every 5 min after adding additional OA/OLA (the sequence of spectra labelled "ligands-1 to ligands-7" corresponds to the time frame 5 to 35 min after addition); inset shows the changes of relative absorbance at two spectral features (315 nm and 500 nm). (c) PL monitoring as in (b); inset shows changes of the PL intensity. (d) Absorption and PL spectra of $CsPbBr_3$ NCs transformed back from intermediate Cs_4PbBr_6 NCs by insertion of $PbBr_2$.

Department of Materials Science and Engineering, and Centre for Functional Photonics (CFP), City University of Hong Kong, 83 Tat Chee Avenue, Kowloon, Hong Kong S.A.R. E-mail: hh@live.cn, andrey.rogach@cityu.edu.hk

† Electronic supplementary information (ESI) available. See DOI: 10.1039/c8ce00911b

cubic $CsPbX_3$ NCs to rhombohedral Cs_4PbX_6 particles, while the opposite reaction recovered $CsPbX_3$ nanoplatelets, instead of cubic $CsPbX_3$ nanocrystals, meaning that the morphology of the originally cubic NCs was not preserved after the transformation cycle. To the best of our knowledge, the directly reversible and fully recovered transformation between the two phases of perovskite NCs has not previously been realized. In the present work, we demonstrate the completely reversible post-synthetic transformation between $CsPbBr_3$ and Cs_4PbBr_6 NCs. The extraction of $PbBr_2$ was trigged by introducing additional ligands to convert $CsPbBr_3$ NCs to Cs_4PbBr_6 NCs. What is more, the obtained Cs_4PbBr_6 NCs can be reverted to $CsPbBr_3$ NCs by reintroducing the $PbBr_2$.

The $CsPbBr_3$ NCs were synthesized according to the hot-injection strategy adopted from previous reports by Kovalenko's group.[4] As illustrated in Fig. 1a, the as-prepared solution of $CsPbBr_3$ NCs shows a sharp PL peak at 515 nm (370 nm excitation wavelength), with a 15 nm Stokes shift and a narrow full width half maxima (FWHM) of 18 nm. Upon addition of the extra ligands, oleylamine (OA) and oleic acid (OLA), the green emitting solution was gradually quenched, eventually transforming into a transparent solution, colorless across the visible spectrum. Corresponding absorption and emission spectra were monitored during the reaction process and are presented in Fig. 1b and c. When extra OA/OLA ligands were introduced dropwise into the $CsPbBr_3$ NCs, the absorbance at 500 nm decreased gradually, indicating the decomposition/disappearance of the $CsPbBr_3$ NCs. Meanwhile, a distinct absorption feature at 315 nm progressively emerged, which is indicative of Cs_4PbBr_6 NC formation, according to the previous reports on bulk Cs_4PbBr_6 powders and films.[35,36] The PL was gradually quenched and accompanied by a slight blue-shift and an increase in the FWHM of the emission peak during the transformation process. After 40 min, the green emission disappeared completely, suggesting the full decomposition of the $CsPbBr_3$ NC structure; the trends in PL spectra matched well in time scale compared with the absorbance changes. To emphasize that the transformation is a cross-over in structures rather than a two-step discrete destruction and replacement we have presented the trends in the PL peak intensity and the evolution of the relative absorbances at two representative spectral positions (315 nm for the characteristic peak of Cs_4PbBr_6 NCs, and 500 nm for the band edge of $CsPbBr_3$ NCs) as a function of time in the insets of Fig. 1b and c. The increase of the absorbance at 315 nm is consistent with and complimentary to the decrease of absorbance at 500 nm, as well as the reduction of the PL peak intensity at 515 nm. It is worth noting that here we choose a suitable concentration (4 mg ml^{-1} of the purified and dried $CsPbBr_3$ NC powder) to illustrate the evolution of the transformation from $CsPbBr_3$ NCs to Cs_4PbBr_6 NCs.

Afterwards, a solution of $PbBr_2$ dissolved in OLA, OA, and toluene was introduced to the above obtained Cs_4PbBr_6 NC solution without any other treatment. Upon the addition of the $PbBr_2$ precursor, the solution started turning turbid and green emission steadily became more pronounced when viewed under a UV lamp. After centrifugation and redispersion in toluene, as shown in Fig. 1d, a large red shift of the absorption spectrum (from displaying a distinct band at 315 nm to showing a band edge step at 500 nm) took place, and a strong and sharp PL peak at 514 nm emerged, with a Stokes shift of 15 nm and FWHM of 22 nm, indicating the transformation from Cs_4PbBr_6 NCs to a luminescent product, which, as we will show below, is $CsPbBr_3$ NCs reformed. Compared with pristine $CsPbBr_3$ NCs, the reproduced luminescent product showed slightly decreased quality in the sharpness of the PL peak (FWHM of 22 nm) after undergoing the forward and reverse transformation processes, but still maintained a high PL QY of 62%, which is fairly close to the original $CsPbBr_3$ NCs PL QY of 79%. The whole transformation process can be observed in the videos provided in the Supporting Information (Videos S1†). This video clearly shows the direct and reversible transformation from green-emitting $CsPbBr_3$ NCs to transparent and colorless Cs_4PbBr_6 NCs, as well as the following inverse transformation without any other treatment or separation. Once transformation was completed, the reproduced $CsPbBr_3$ NC solution showed strong green emission again.

The TEM images in Fig. 2 illustrate the change of morphology during the transformation process between $CsPbBr_3$ NCs and Cs_4PbBr_6 NCs, with high-resolution TEM (HRTEM) images presented in the respective insets. As shown in Fig. 2a, the as-prepared $CsPbBr_3$ NCs are highly uniform, monodisperse and possess a cubic shape with an average edge size of 10 nm. After the addition of extra ligands, the morphology of the samples dramatically changed to relatively monodisperse, frequently hexagonal in cross-section, NCs with an average edge length of 18 nm (Fig. 2b). If we approximate the NCs before and after transformation as discrete

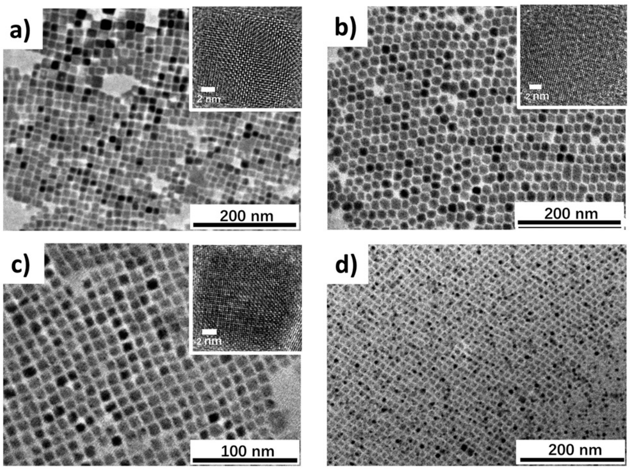

Fig. 2 TEM images of (a) as-prepared $CsPbBr_3$ NCs, (b) Cs_4PbBr_6 NCs transformed from $CsPbBr_3$ NCs after addition of extra OA/OLA ligands, (c) and (d) $CsPbBr_3$ NCs reshaped reversibly from Cs_4PbBr_6 NCs (pictures are taken on different parts of the grid and at two different magnifications). Insets in (a) to (c) are HRTEM images of the respective single particles.

spheres, and take Cs atom numbers per particle to remain the same before and after transformation, and take the Pb–Pb distance between neighboring $[PbX_6]^{4-}$ octahedra in changing from corner-sharing in $CsPbBr_3$ to isolated in Cs_4PbBr_6, to shift from 5.9 Å to 10 Å,[41] we can then calculate the particle dilation to be 1.7 times, which is in good agreement with our observed size change from 10 nm for $CsPbBr_3$ NCs to 18 nm for Cs_4PbBr_6 NCs. Markedly, as shown in Fig. 2c, the introduction of $PbBr_2$ results in the reshaping of the NCs from a hexagonoid shape back to regular cubic NCs. Although the NCs underwent a shape transformation, the overall size after reformation of the cubic NCs was almost preserved, with an average edge size of 9 nm on completion of the whole cycle. The slight emission quality loss, seen in the PL spectra in Fig. 1d as a slightly extended short wavelength tail, is correlated with the morphological transformation from hexagonal shape to cubic NCs, which leaves behind some smaller debris, as shown in Fig. 2d. The overall shrinkage in the size of the NCs from 10 nm to 9 nm edge lengths following this treatment suggests the transformation may be accompanied by considerable reorganization of the lattice when going from $CsPbBr_3$ to Cs_4PbBr_6, then back to $CsPbBr_3$ resulting in some loss of the original material.

To confirm the crystal structure and phase purity during the transformation, we characterized the products before, during and after treatment by X-ray diffraction (XRD). Fig. 3 shows the XRD patterns of as-prepared $CsPbBr_3$ NCs, the products collected during reaction of extra OA/OLA ligands (measured every 3 min), and products collected after treatment of $PbBr_2$. Peaks of the original $CsPbBr_3$ NCs have been assigned to the cubic phase following our previous report[42] and that by Kovalenko's group.[4] The structural evolution of these NCs upon the addition of extra ligands was monitored. The characteristic peaks of $CsPbBr_3$ gradually disappeared, and some new peaks matching the reference #732478 pattern for the hexagonal Cs_4PbBr_6 phase became more obvious.[35,36] Both phases coexist from 0 min to 9 min. Finally, after 12 min, the peaks corresponding to the $CsPbBr_3$ NCs vanished and only the Cs_4PbBr_6 phase remained. Then, following the introduction of $PbBr_2$, the crystal structure transformed back to $CsPbBr_3$ NCs. Peaks can be attributed to reference pattern #29073 for the cubic phase of $CsPbBr_3$ NCs, although with broader peaks compared to the pristine $CsPbBr_3$ NCs, indicating slightly smaller NC sizes. Additionally, XRD reference patterns of the precursors (#310679 for $PbBr_2$ and #050588 for CsBr) and the absence of their characteristic lines in intermediate patterns can further rule out the consideration of decomposition or degradation of NCs back to precursors during the transformation process. As a whole, the XRD patterns confirm the crystal phase of $CsPbBr_3$ NCs and Cs_4PbBr_6 NCs during the reversible transformation. Both the as-prepared $CsPbBr_3$ NCs and the finally obtained $CsPbBr_3$ NCs were in the cubic phase and the intermediate Cs_4PbBr_6 NCs were in the hexagonal phase.

The transformation in morphology and crystal structure are evidenced by TEM and XRD, and these are coincident with the evolution of absorption and PL spectra. From these data, we can infer the reversible transformation process between $CsPbBr_3$ NCs and Cs_4PbBr_6 NCs, which is outlined in

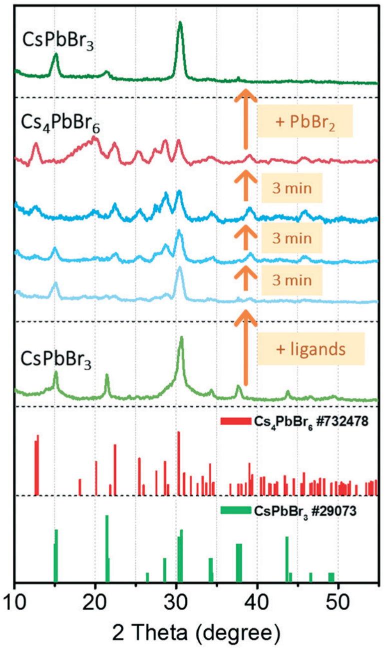

Fig. 3 XRD pattern evolution during the reversible transformation from as-prepared $CsPbBr_3$ NCs to Cs_4PbBr_6 NCs, and then transformed back to $CsPbBr_3$ NCs. Both the as-prepared $CsPbBr_3$ NCs and the finally obtained $CsPbBr_3$ NCs were in the cubic phase, the intermediate Cs_4PbBr_6 NCs were in an hexagonal phase. The XRD patterns during the transformation process were monitored every 3 minutes upon adding extra OA/OLA ligands and revealed the coexistence and peak change of both $CsPbBr_3$ NCs and Cs_4PbBr_6 NCs. XRD references patterns #732478 for Cs_4PbBr_6 and #29073 for $CsPbBr_3$ are shown as line spectra.

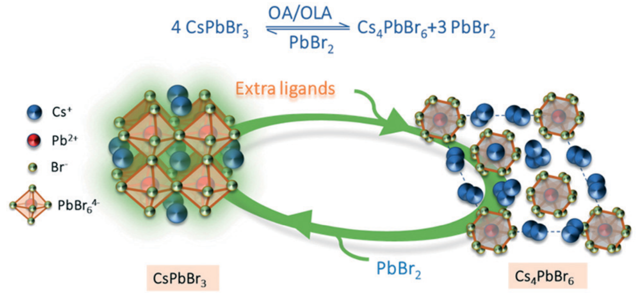

Fig. 4 Structural models demonstrating the reversible transformation between luminescent $CsPbBr_3$ and non-luminescent Cs_4PbBr_6 NCs. Cs_4PbBr_6 NCs are obtained after addition of extra ligands (OA/OLA) into the original $CsPbBr_3$ NCs solution. Reversibly, the Cs_4PbBr_6 NCs are transformed back to strongly fluorescent $CsPbBr_3$ NCs *via* an insertion reaction with additional $PbBr_2$. The $CsPbBr_3$ NCs structure is characterized by corner sharing $[PbX_6]^{4-}$ octahedra with Cs^+ cations filling the voids created by four neighboring $[PbX_6]^{4-}$ octahedra. In the Cs_4PbBr_6 NCs structure, adjacent $[PbBr_6]^{4-}$ octahedra do not share any corners and are completely decoupled in all directions. Thus, excess $PbBr_2$ can be integrated into the crystal structure of Cs_4PbBr_6 NCs to form compactly arranged $CsPbBr_3$ NCs.

Fig. 4. The forward reaction is triggered by extra ligands OA and OLA. Upon the addition of these ligands, stripping of $PbBr_2$ occurs because they can break the equilibrium of the dynamic surface ligand shell, offering the opportunity for ligand desorption, leading to strong binding with surface $PbBr_2$ and subsequent extraction of these units from the previous cubic structure.[38,39] Eventually, after sufficient extraction, the formation of Cs_4PbBr_6 NCs is achieved. TEM and X-ray diffraction indicate that all the NCs in the final forward product have the hexagonal Cs_4PbBr_6 phase and no remaining $CsPbBr_3$ phase was present. Cs_4PbBr_6 NCs have been previously regarded as a $PbBr_2$-deficient or $PbBr_2$-depleted structure,[38] which supports our hypothesis of extraction of $PbBr_2$ from another aspect. For the backwards reaction, the hexagonal Cs_4PbBr_6 NCs are converted back to cubic structured $CsPbBr_3$ NCs through the insertion reaction of $PbBr_2$, which is supported by the ionic nature of Cs_4PbBr_6. In Cs_4PbX_6, the $[PbX_6]^{4-}$octahedra are completely decoupled in all lattice directions. In contrast, $CsPbBr_3$ possesses a higher symmetry, simple cubic structure with corner sharing $[PbX_6]^{4-}$ octahedra with the Cs^+ cations filling the voids created by four neighboring $[PbX_6]^{4-}$ octahedra. Thus, excess $PbBr_2$ can be integrated into the crystal structure of Cs_4PbBr_6 NCs to form compactly arranged $CsPbBr_3$ NCs.

In summary, we have realized a reversible transformation between $CsPbBr_3$ and Cs_4PbBr_6 NCs through simple treatments with extra OA/OLA ligands or $PbBr_2$, which is governed by an extraction or insertion of $PbBr_2$. This transformation is yet the first report of direct reversibility between $CsPbBr_3$ NCs and Cs_4PbBr_6 NCs where the cubic morphology of the $CsPbBr_3$ NCs before and after the whole cycle is preserved. The study not only allows for understanding the detailed structural characteristics of $CsPbBr_3$ NCs and Cs_4PbBr_6 NCs, but also for the flexible reorganization of lattices in perovskite systems. The possibility of reversible transformation indicates that the perovskite crystal structure may potentially withstand multiple reorganization cycles tailored to the desired application.

Experimental section

Materials

$PbBr_2$ (98%, Aldrich), Cs_2CO_3(99.99%, Aldrich), oleylamine (98%, OA, Aldrich), oleic acid (90%, OLA, Aldrich), 1-octadecene (90%, Aldrich), toluene (99.7% GC, Sigma-Aldrich). OA and OLA were dried for 1 h under vacuum at 100 °C before use. The other chemicals were used as received.

$CsPbBr_3$ NCs synthesis and purification

Cs-oleate was synthesized by reaction of Cs_2CO_3 (0.16 g) with OA (0.5 mL) in octadecene (10 mL) and pre-heated to 100 °C before injection. $PbBr_2$ (0.282 mmol) and 7.5 mL of octadecene were loaded into a 100 mL 2-neck flask, dried under vacuum at 120 °C for 1 h, and mixed with vacuum dried OLA (0.75 mL) and OA (0.75 mL) under a N_2 atmosphere. The temperature was raised to 180 °C and 0.6 mL of Cs-oleate solution was swiftly injected. After 5 s, the reaction was quenched by placing the mixture into an ice water bath. The NCs were precipitated by centrifugation at 5000 rpm and re-dispersed in 5 mL toluene, followed by a subsequent centrifugation at 10 000 rpm and re-dispersion in toluene for further use.

Transformation of $CsPbBr_3$ NCs to Cs_4PbBr_6 NCs *via* extra ligand addition

For a typical reaction, 100 μL OA and 100 μL OLA were added dropwise into 2 mL of $CsPbBr_3$ NC solution (4 mg mL^{-1}) under stirring. The solution was quenched totally within 30 min, transforming into a transparent non-luminescent solution. The transformation time was dependent upon the concentration of the $CsPbBr_3$ NC solution, as well as the amount of extra ligand added.

Transformation of Cs_4PbBr_6 NCs back to $CsPbBr_3$ NCs with added $PbBr_2$ precursor

100 μL of $PbBr_2$ precursor was injected (1 mmol $PbBr_2$ dissolved in 0.5 mL toluene, 0.25 mL OA and 0.25 mL OLA) into 2 mL of Cs_4PbBr_6 NC solution heated at 80 °C under stirring. Upon injection, the solution started turning green and turbid. After 30 min, the resulting solution was cooled down with an ice water bath and subsequently centrifuged at 5000 rpm and re-dispersed in 5 mL toluene for further analysis.

Characterization

PL spectra were measured on a Cary Eclipse (Varian) spectrometer. Absorption spectra were recorded using a Cary 50 UV-vis spectrophotometer (Varian). Powder X-ray diffraction (XRD) patterns were taken on a Philips X-Pert X-ray diffractometer using Cu Kα radiation (λ = 1.5418 Å). Transmission electron microscopy (TEM) was carried out on a Philips CM-20 instrument. The PL quantum yield, defined as the ratio between photons emitted and absorbed by the sample, was determined by an absolute method using an integrating sphere with its inner face coated with BENFLEC® (Edinburgh Instruments), fitted to an Edinburgh Instruments FLS 920 spectrofluorimeter.

Conflicts of interest

There are no conflicts to declare.

Acknowledgements

This work was supported by the Research Grants Council of Hong Kong S.A.R. (CityU11337616).

References

1 L. C. Schmidt, A. Pertegas, S. Gonzalez-Carrero, O. Malinkiewicz, S. Agouram, G. Minguez Espallargas, H. J. Bolink, R. E. Galian and J. Perez-Prieto, *J. Am. Chem. Soc.*, 2014, **136**, 850–853.

2 H. Huang, L. Polavarapu, J. A. Sichert, A. S. Susha, A. S. Urban and A. L. Rogach, *NPG Asia Mater.*, 2016, **8**, e328.

3 H. Huang, J. Raith, S. V. Kershaw, S. Kalytchuk, O. Tomanec, L. Jing, A. S. Susha, R. Zboril and A. L. Rogach, *Nat. Commun.*, 2017, **8**, 996.

4 L. Protesescu, S. Yakunin, M. I. Bodnarchuk, F. Krieg, R. Caputo, C. H. Hendon, R. X. Yang, A. Walsh and M. V. Kovalenko, *Nano Lett.*, 2015, **15**, 3692–3696.

5 Y. Tong, B. J. Bohn, E. Bladt, K. Wang, P. Muller-Buschbaum, S. Bals, A. S. Urban, L. Polavarapu and J. Feldmann, *Angew. Chem., Int. Ed.*, 2017, **56**, 13887–13892.

6 Q. A. Akkerman, G. Raino, M. V. Kovalenko and L. Manna, *Nat. Mater.*, 2018, 29459748.

7 F. Zhang, H. Zhong, C. Chen, X. G. Wu, X. Hu, H. Huang, J. Han, B. Zou and Y. Dong, *ACS Nano*, 2015, **9**, 4533–4542.

8 C. Zhou, Y. Tian, M. Wang, A. Rose, T. Besara, N. K. Doyle, Z. Yuan, J. C. Wang, R. Clark, Y. Hu, T. Siegrist, S. Lin and B. Ma, *Angew. Chem., Int. Ed.*, 2017, **56**, 9018–9022.

9 B. Luo, Y. C. Pu, S. A. Lindley, Y. Yang, L. Lu, Y. Li, X. Li and J. Z. Zhang, *Angew. Chem., Int. Ed.*, 2016, **55**, 8864–8868.

10 D. Zhang, Y. Yu, Y. Bekenstein, A. B. Wong, A. P. Alivisatos and P. Yang, *J. Am. Chem. Soc.*, 2016, **138**, 13155–13158.

11 S. Sun, D. Yuan, Y. Xu, A. Wang and Z. Deng, *ACS Nano*, 2016, **10**, 3648–3657.

12 A. Swarnkar, R. Chulliyil, V. K. Ravi, M. Irfanullah, A. Chowdhury and A. Nag, *Angew. Chem.*, 2015, **127**, 15644–15648.

13 J. Li, L. Xu, T. Wang, J. Song, J. Chen, J. Xue, Y. Dong, B. Cai, Q. Shan, B. Han and H. Zeng, *Adv. Mater.*, 2017, **29**, 1603885.

14 D. N. Dirin, L. Protesescu, D. Trummer, I. V. Kochetygov, S. Yakunin, F. Krumeich, N. P. Stadie and M. V. Kovalenko, *Nano Lett.*, 2016, **16**, 5866–5874.

15 H. Huang, M. I. Bodnarchuk, S. V. Kershaw, M. V. Kovalenko and A. L. Rogach, *ACS Energy Lett.*, 2017, **2**, 2071–2083.

16 X. Zhang, X. Bai, H. Wu, X. Zhang, C. Sun, Y. Zhang, W. Zhang, W. Zheng, W. W. Yu and A. L. Rogach, *Angew. Chem., Int. Ed.*, 2018, **57**, 3337–3342.

17 H. Huang, B. Chen, Z. Wang, T. F. Hung, A. S. Susha, H. Zhong and A. L. Rogach, *Chem. Sci.*, 2016, **7**, 5699–5703.

18 R. Yuan, L. Shen, C. Shen, J. Liu, L. Zhou, W. Xiang and X. Liang, *Chem. Commun.*, 2018, **54**, 3395–3398.

19 H. Huang, H. Lin, S. V. Kershaw, A. S. Susha, W. C. Choy and A. L. Rogach, *J. Phys. Chem. Lett.*, 2016, **7**, 4398–4404.

20 X. Zhang, H. Liu, W. Wang, J. Zhang, B. Xu, K. L. Karen, Y. Zheng, S. Liu, S. Chen, K. Wang and X. W. Sun, *Adv. Mater.*, 2017, **29**, 1606405.

21 J. Pan, L. N. Quan, Y. Zhao, W. Peng, B. Murali, S. P. Sarmah, M. Yuan, L. Sinatra, N. M. Alyami, J. Liu, E. Yassitepe, Z. Yang, O. Voznyy, R. Comin, M. N. Hedhili, O. F. Mohammed, Z. H. Lu, D. H. Kim, E. H. Sargent and O. M. Bakr, *Adv. Mater.*, 2016, **28**, 8718–8725.

22 H. Huang, A. S. Susha, S. V. Kershaw, T. F. Hung and A. L. Rogach, *Adv. Sci.*, 2015, **2**, 1500194.

23 H. C. Wang, S. Y. Lin, A. C. Tang, B. P. Singh, H. C. Tong, C. Y. Chen, Y. C. Lee, T. L. Tsai and R. S. Liu, *Angew. Chem., Int. Ed.*, 2016, **55**, 7924–7929.

24 Q. Zhou, Z. Bai, W. G. Lu, Y. Wang, B. Zou and H. Zhong, *Adv. Mater.*, 2016, **28**, 9163–9168.

25 H. Huang, Q. Xue, B. Chen, Y. Xiong, J. Schneider, C. Zhi, H. Zhong and A. L. Rogach, *Angew. Chem., Int. Ed.*, 2017, **56**, 9571–9576.

26 W. Deng, X. Zhang, L. Huang, X. Xu, L. Wang, J. Wang, Q. Shang, S. T. Lee and J. Jie, *Adv. Mater.*, 2016, **28**, 2201–2208.

27 L. Gao, K. Zeng, J. Guo, C. Ge, J. Du, Y. Zhao, C. Chen, H. Deng, Y. He, H. Song, G. Niu and J. Tang, *Nano Lett.*, 2016, **16**, 7446–7454.

28 Y. C. Kim, K. H. Kim, D. Y. Son, D. N. Jeong, J. Y. Seo, Y. S. Choi, I. T. Han, S. Y. Lee and N. G. Park, *Nature*, 2017, **550**, 87–91.

29 H. T. Wei, Y. J. Fang, P. Mulligan, W. Chuirazzi, H. H. Fang, C. C. Wang, B. R. Ecker, Y. L. Gao, M. A. Loi, L. Cao and J. S. Huang, *Nat. Photonics*, 2016, **10**, 333–339.

30 C. Zhang, B. Wang, W. Li, S. Huang, L. Kong, Z. Li and L. Li, *Nat. Commun.*, 2017, **8**, 1138.

31 X. Li, Y. Wang, H. Sun and H. Zeng, *Adv. Mater.*, 2017, **29**, 1701185.

32 S. Yakunin, L. Protesescu, F. Krieg, M. I. Bodnarchuk, G. Nedelcu, M. Humer, G. De Luca, M. Fiebig, W. Heiss and M. V. Kovalenko, *Nat. Commun.*, 2015, **6**, 8056.

33 A. Pan, B. He, X. Fan, Z. Liu, J. J. Urban, A. P. Alivisatos, L. He and Y. Liu, *ACS Nano*, 2016, **10**, 7943–7954.

34 J. De Roo, M. Ibanez, P. Geiregat, G. Nedelcu, W. Walravens, J. Maes, J. C. Martins, I. Van Driessche, M. V. Kovalenko and Z. Hens, *ACS Nano*, 2016, **10**, 2071–2081.

35 Q. A. Akkerman, S. Park, E. Radicchi, F. Nunzi, E. Mosconi, F. De Angelis, R. Brescia, P. Rastogi, M. Prato and L. Manna, *Nano Lett.*, 2017, **17**, 1924–1930.

36 F. Palazon, C. Urso, L. De Trizio, Q. Akkerman, S. Marras, F. Locardi, I. Nelli, M. Ferretti, M. Prato and L. Manna, *ACS Energy Lett.*, 2017, **2**, 2445–2448.

37 H. Wu, S. Xu, H. Shao, L. Li, Y. Cui and C. Wang, *Nanoscale*, 2017, **9**, 16858–16863.

38 Z. Liu, Y. Bekenstein, X. Ye, S. C. Nguyen, J. Swabeck, D. Zhang, S. T. Lee, P. Yang, W. Ma and A. P. Alivisatos, *J. Am. Chem. Soc.*, 2017, **139**, 5309–5312.

39 F. Palazon, G. Almeida, Q. A. Akkerman, L. De Trizio, Z. Dang, M. Prato and L. Manna, *Chem. Mater.*, 2017, **29**, 4167–4171.

40 T. Udayabhaskararao, L. Houben, H. Cohen, M. Menahem, I. Pinkas, L. Avram, T. Wolf, A. Teitelboim, M. Leskes, O. Yaffe, D. Oron and M. Kazes, *Chem. Mater.*, 2018, **30**, 84–93.

41 Q. A. Akkerman, A. L. Abdelhady and L. Manna, *J. Phys. Chem. Lett.*, 2018, **9**, 2326–2337.

42 S. Fang, G. Li, H. Li, Y. Lu and L. Li, *Chem. Commun.*, 2018, **54**, 3863–3866.